haematologica
Journal of the Ferrata Storti Foundation

Molecular measurable residual disease by immunoglobulin gene rearrangements on circulating tumor DNA predicts outcome in diffuse large B-cell lymphoma

by Roberta Soscia, Giovanni Manfredi Assanto, Irene Della Starza, Riccardo Moia, Donatella Talotta, Vittorio Bellomarino, Teresa Bellissimo, Marco Antonacci, Luigi Petrucci, Gianluca Gaidano, Anna Guarini, Maurizio Martelli, Alice Di Rocco, Robin Foà and Ilaria Del Giudice

Received: July 24, 2024.
Accepted: December 13, 2024.

Citation: Roberta Soscia, Giovanni Manfredi Assanto, Irene Della Starza, Riccardo Moia, Donatella Talotta, Vittorio Bellomarino, Teresa Bellissimo, Marco Antonacci, Luigi Petrucci, Gianluca Gaidano, Anna Guarini, Maurizio Martelli, Alice Di Rocco, Robin Foà and Ilaria Del Giudice. Molecular measurable residual disease by immunoglobulin gene rearrangements on circulating tumor DNA predicts outcome in diffuse large B-cell lymphoma.
Haematologica. 2024 Dec 19. doi: 10.3324/haematol.2024.286331 [Epub ahead of print]

Molecular measurable residual disease by immunoglobulin gene rearrangements on circulating tumor DNA predicts outcome in diffuse large B-cell lymphoma

*Roberta Soscia,[1] *Giovanni Manfredi Assanto,[1] Irene Della Starza,[2] Riccardo Moia,[3] Donatella Talotta,[3] Vittorio Bellomarino,[1] Teresa Bellissimo,[1] Marco Antonacci,[1] Luigi Petrucci,[1] Gianluca Gaidano,[3] Anna Guarini,[4] Maurizio Martelli,[1] Alice Di Rocco,[1] Robin Foà,[1] and Ilaria Del Giudice[1]

[1]Hematology, Department of Translational and Precision Medicine, Sapienza University, Rome, Italy
[2]AIL Roma Odv, Rome, Italy
[3]Division of Hematology, Department of Translational Medicine, University of Eastern Piedmont, Novara, Italy
[4]Department of Molecular Medicine, Sapienza University, Rome, Italy

Contributions

*RS and GMA contributed equally as co-first authors.
IDG, ADR and RF conceived and designed the study; RM, DT, MA, LP, ADR, MM, provided study materials of patients; RS, GMA, IDS, VB performed the NGS-IG screening and MRD analysis; TB managed the clinical database; RS and GMA performed bioinformatic analysis; RS, GMA, IDS, ADR, GG, MM, AG, RF and IDG contributed to data interpretation; RS, GMA and IDG wrote the manuscript; all authors contributed to manuscript revision and its final approval.

Running head

IG ctDNA MRD refines DLBCL treatment response

Corresponding author

Ilaria Del Giudice, e-mail: delgiudice@bce.uniroma1.it, phone: +39-06-441639822, fax: +39-06-44241984; Hematology, Sapienza University of Rome, via Benevento 6, 00161 Rome, Italy

Data sharing statement

The data that support the findings of this study are available from the corresponding author upon reasonable request.

Conflict-of-interest disclosure

IDG received honoraria for participation in advisory board and educational events from AstraZeneca, Janssen, Roche, and Takeda. ADR received honoraria for participation in advisory board and educational events from Janssen, Roche, Takeda, AbbVie, Gilead/Kite, Incyte, and Lilly. RM received honoraria for participation in advisory board from BeiGene, AbbVie, and Johnson & Johnson. GG received honoraria for participation in advisory board and/or speakers bureaus from AbbVie, AstraZeneca, BeiGene, Hikma, Incyte, Johnson & Johnson, Lilly, and Roche. MM received research support from Alexion; and received honoraria for participation in advisory board and/or speakers bureaus from Roche, Gilead, Novartis, Takeda, Incyte, Janssen, BMS, BeiGene, and Lilly. The remaining authors have nothing to disclose.

Funding

This work was supported by Associazione Italiana per la Ricerca sul Cancro (AIRC) Special 5x1000 Program “Metastatic disease: the key unmet need in oncology” (21198), Milan (Italy) to RF and GG, and bando di Ateneo Sapienza (RM11816435B1A7A0) to ADR.

ABSTRACT

In diffuse large B-cell lymphoma (DLBCL) treatment response relies on imaging. We investigated the potential value of molecular measurable residual disease (MRD) on circulating tumor DNA (ctDNA) to predict patient outcomes.

We retrospectively evaluated 73 patients. Analyses were conducted on 57 tumor biopsies, based on sample availability. At baseline, next-generation sequencing was used to detect clonal immunoglobulin (IG) gene rearrangements on tumor biopsies and ctDNA. MRD monitoring was applied by tracking the IG clones in ctDNA samples collected during treatment (interim) and at the end of treatment (EOT). MRD results were correlated with clinical data and radiologic disease assessment. Before treatment, clonal IG were found in 91.2% (52/57) of tumor biopsies and in 93.2% (68/73) of ctDNA samples. In paired samples, the same clonotype was found in 69.2% (36/52) of cases. At the interim analysis, ctDNA MRD was negative in 32/45 evaluable patients and positive in 13/45, correlating significantly with progression-free survival (PFS) (78.1% MRD- *vs* 30.8% MRD+; $p<0.0001$) after a median follow-up of 40 months. Moreover, ctDNA MRD could stratify prognosis of 27 patients in partial response ($p=0.018$). At EOT, ctDNA MRD was negative in 37/47 patients and positive in 10/47 (PFS 83.8% MRD- *vs* 0% MRD+; $p<0.0001$). All MRD+ patients in complete metabolic response relapsed ($p<0.0001$). At multivariate analysis, MRD at EOT independently predicted PFS and overall survival.

Monitoring IG-based ctDNA MRD during and after treatment predicts DLBCL patient outcome. This non-invasive method should be implemented in risk-adapted clinical trials and validated as a treatment decision-making tool.

INTRODUCTION

Diffuse large B-cell lymphoma (DLBCL), the most frequent non-Hodgkin lymphoma (NHL) in the Western world, is a heterogeneous disease with genetic diversity and variable outcomes.[1-4] It arises from a mature clonal B-cell population that exhibits clonal immunoglobulin (IG) gene rearrangements. The current standard to monitor DLBCL response to therapy relies on the macro-estimation of tumor reduction by computed tomography (CT) or positron emission tomography/CT (PET/CT) scans, that can show suboptimal specificity.[5] In the last few years, the therapeutic scenario of DLBCL has changed, especially in the relapsed/refractory (R/R) setting with the introduction of novel targeted agents, namely bispecific monoclonal antibodies and cellular-based immunotherapies such as the chimeric antigen receptor T (CAR-T) cell therapy, leading to higher rates of complete responses and longer survival.[6-8] Consequently, the possibility of monitoring measurable residual disease (MRD) has become more relevant to further personalize treatment. One major obstacle is the absence of circulating neoplastic cells. The development of robust techniques, including next-generation sequencing (NGS), together with the discovery of circulating tumor DNA (ctDNA), shed into the bloodstream by tumor cells undergoing apoptosis, have opened the door to leukemia-like research in NHL.[9-13] Some research groups have investigated the relationship between baseline levels of ctDNA and conventional markers of tumor burden and its role as a prognostic biomarker.[14-18] More importantly, ctDNA has been used as a non-invasive tool to track recurrently mutated genes in DLBCL, allowing capture of the mutational landscape beyond the intra-tumoral heterogeneity (i.e., liquid biopsy), to monitor the molecular disease during and after treatment, and to evaluate clonal evolution.[9-13,16-18]

Disease-specific clonal rearrangement of the IG genes can be identified on the diagnostic tumor tissue using a single NGS assay that utilizes universal primers for all possible rearrangements. The specific clonotype of each patient can subsequently be tracked for disease monitoring.[19-22]

The aim of this study was to evaluate if ctDNA MRD monitoring based on IG gene rearrangements may improve DLBCL treatment response assessment and outcome prediction. The results obtained indicate that ctDNA monitoring may indeed be proposed as a decision-making tool to guide lymphoma treatment in the future.

METHODS

Patients and samples

We performed a multicenter retrospective study on a cohort of 73 consecutive newly diagnosed DLBCL patients (41 from Rome and 32 from Novara), enrolled between September 2015 and March 2021. Inclusion criteria were: (1) age ≥18 years; (2) histological diagnosis of DLBCL

(including DLBCL not otherwise specified, NOS; transformed indolent B-cell lymphoma; high-grade B cell lymphoma with rearrangements of MYC and BCL2 and/or BCL6; excluding primary mediastinal B-cell lymphoma); (3) previously untreated patients eligible for curative treatment. Patients were all treated according to guidelines in force at the time of diagnosis, with rituximab plus cyclophosphamide, doxorubicin, vincristine, and prednisone (R-CHOP) or R-CHOP-like regimens.[23,24] The following biological materials were collected: diagnostic formalin-fixed paraffin embedded (FFPE) tumor biopsies (for genomic DNA, gDNA) and 30 ml of peripheral blood (PB) for ctDNA before the start of treatment, throughout the first three cycles of therapy (cycle 2 day 1, C2D1, for the Novara cohort, and cycle 4 day 1, C4D1, for the Rome cohort), and at the end of treatment (EOT). Early (mid-treatment) and final (EOT) disease response were assessed by CT and PET/CT, respectively. Interim CT scans were performed between three to four cycles and interpreted according to Cheson's criteria.[5] Response to treatment was defined according to the Lugano criteria.[25] Relapse within 12 months from treatment initiation was considered early relapse.
Patients provided written informed consent, the study respected the Helsinki Declaration principles and was approved by the ethical committee of AOU Policlinico Umberto I, Rome (Prot n. 877/19 rif. CE 5629, AIRC 21198). The endpoints of the study were: 1) to test the applicability of NGS for IG heavy (IGH) and kappa light (IGK) chain gene rearrangements in FFPE diagnostic tumor biopsies and ctDNA extracted from PB; 2) to explore if tracking clonal IGH/IGK rearrangements by NGS can be a non-invasive method to study MRD in longitudinal ctDNA samples during and after treatment; 3) to study the correlation of IG-based ctDNA MRD with clinical data and radiologic disease assessment of early (CT) and final response (PET/CT).

Experimental procedure

FFPE diagnostic tissue from lymph node biopsies or from other extra nodal tissue excisions was available in 57 patients. In the remaining 16 cases, the diagnostic biopsy was not available. All samples were sectioned in 3-4 μm thick sections. gDNA was extracted from FFPE tissue with the automated Maxwell RSC DNA FFPE Kit (Promega, Madison, WI), according to the manufacturer's instructions. DNA amounts were assessed using the Qubit dsDNA BR Assay Kit (Thermo Fisher Scientific, Waltham, MA). The Specimen Control Size Ladder master mix (Invivoscribe Inc, San Diego, CA) was then used to ensure that the quantity and quality of sample DNA was adequate. A standardized approach was used to extract cell-free DNA (cfDNA) from the plasma of 73 patients (Supplementary Data).[26] Plasma samples collected from 7 healthy donors were also analyzed (Supplementary Data).

The LymphoTrack IGH framework region (FR) 1/2/3 and IGK assay panels (Invivoscribe) were used to analyze the diagnostic FFPE and plasma samples aiming at detecting clonotypic rearrangements and at identifying the DNA sequence specific for each clonal gene rearrangement. Initially, the samples were analyzed for IGH rearrangements. Cases without a detectable clonal sequence through IGH-targeted testing were subsequently tested for IGK rearrangements. IGK was not routinely tested in plasma due to the greater reliability of the IGH marker compared to IGK for MRD monitoring.[27] It was only tested in the 16 cases for which a biopsy was unavailable and in case of a clonality discordance between tumor biopsy and plasma.

Identification of clonality followed a three-step workflow: (1) PCR amplification; (2) NGS; and (3) bioinformatics analysis (LymphoTrack Dx MiSeq software v2.4.3). Multiplexed libraries were sequenced using 500-bp paired-end runs on a MiSeq sequencer (Illumina, San Diego, CA), aiming at achieving 1 million reads per sample.

The lymphoma-derived sequences were then used as target to assess MRD on ctDNA.[26,28] A more detailed description of the methods used for MRD detection can be found in the Supplementary Methods. In case of clonal marker discordancy between plasma and tumor biopsy, the sequencing data from both compartments were examined using a diverse bioinformatic analysis to determine if the detected clonal sequences were present in matched tissues at lower burdens than the clonal definition.

Statistical analysis

Univariate analysis was performed to assess normal distribution of characteristics between the two centers. Pearson correlation Student T test and Mann Whitney were used to compare continuous variables, and a Chi-square test was performed to correlate ctDNA clonotype identification with categorical variables.

Survival probabilities were estimated using the Kaplan-Meier method; the log-rank test was used to determine the significance of the difference between Kaplan-Meier curves. Two survival endpoints were considered: progression-free survival (PFS), where an event was defined as progression or relapse from diagnosis, and overall survival (OS), where an event was defined as death resulting from any cause from diagnosis. Regression analysis of multiple covariates was conducted using the Cox proportional hazard model. Hazard ratios (HR) and corresponding 95% confidence intervals (CI) are reported. All *p* values were two-tailed. Statistical analyses were carried out using SPSS Statistics v.25.0 (IBM Corp., Armonk, NY).

RESULTS

Patients' population

A series of 73 consecutive untreated DLBCL patients were enrolled and followed after treatment with R-CHOP/R-CHOP-like regimens. Overall, two patients showed refractory disease during treatment, 18 had a relapse after a median of 20.5 months from the start of treatment (range, 7.5-52), of whom 14 (78%) occurred within 24-months and 6 (33%) experienced an early relapse (occurring within 12 months from the start of treatment). Two patients (2.7%) had a central nervous system (CNS) involvement at the time of systemic relapse after 8 and 21 months from the start of treatment, respectively. All relapses were documented through imaging and clinical assessment, in this series no patient underwent a new biopsy.

After a median follow-up of 40 months (range 1-72), OS was 76.6% (17/73) and PFS 72.6% (20/73).

Thirteen of the 20 R/R patients (65%) died of disease progression. Four deaths were observed in the disease-free group of patients (COVID-19 1, stroke 1, second malignancy 1 and comorbidities 1).

At univariate analysis, the following risk factors were confirmed as clinical predictors of PFS: ECOG PS (p=0.05), IPI score (p=0.024) and stage (p=0.011).

Patients' characteristics are listed in Table 1A, patients' outcome in Table 1B.

IG analysis of tumor biopsy

The FFPE tumor biopsy available in 57/73 DLBCL patients was subjected to IG-NGS with the IGH (FR1/2/3) and IGK assay panels. At least one dominant tumor-specific clonotype was identified in 91.2% of cases (52/57). Forty-one patients (71.9%) had clonal sequences detectable by IGH primers and 11 (19.3%) by IGK primers. In the remaining 5 cases (8.8%), both IGH and IGK clonality assessment showed polyclonal patterns and an index clone was not identified; in these cases with undetectable clonality, DNA was suboptimal in terms of quantity and quality (highly fragmented).

Of the 52 patients with a tumor-specific clonotype, most (65%, 34/52) were successfully characterized by one assay (1 for IGH-FR1, 12 for IGH-FR2, 10 for IGH-FR3 and 11 for IGK), 13 (25%) were clonal for two assays (12 for IGH-FR2/3 and 1 for IGH-FR1/2) and 5 (10%) were clonal for all three IGH assays (FR1/2/3).

Of these 52 cases, 43 (82.7%, 43/52) showed a unique clonal sequence, 6 (11.5%) showed two unrelated clonal sequences with different IGH and IGK V-J gene segment usage, while 3 cases (5.8%) showed two clonal sequences with identical IGH V-J segment usage but differing by ≥2 nucleotide substitutions, with different CDR3 regions.

Clonal detection was independent from biopsy site and extra nodal disease involvement at PET/CT.

Pre-treatment ctDNA IG analysis

Basal plasma samples were collected in close temporal proximity of the tumor biopsy, before starting treatment. The cfDNA of the 73 DLBCL patients was subjected to IG-NGS with IGH (FR2/FR3) and IGK assay panels. The median plasma cfDNA concentration was 10 ng/mL (range 1.89-211) and ctDNA clonality was detected in 68/73 patients (93.2%). Most plasmatic ctDNAs (75%, 51/68) were clonal by one assay (20 for IGH-FR2, 20 for IGH-FR3 and 11 for IGK), 14 (21%, 14/68) were clonal by two assays (13 for IGH-FR2/3 and 1 for IGH-FR3 and IGK) and 3 (4%, 3/68) were clonal by three assays (IGH-FR2/3 and IGK).

The clonal IG rearrangements identified in ctDNA at diagnosis were then matched with lymphoma-specific clonotype identified in the paired tumor biopsy of the 52 patients. Identical IG markers were found in 36/52 cases (69.2%). In 11/52 cases (21.2%) a different clonal marker was found in the plasma compared to the tumor biopsy and in 5/52 (9.6%) cases no clonality was detected in the ctDNA (Supplementary Table S1). Among the 11 discordant cases, 9/11 (82%) had IGH rearrangements and only 2/11 (18%) IGK rearrangements. No case showed double IGH-IGK rearrangements. Moreover, the clonal sequences detected in ctDNA were absent in the matched tumor tissue, even at lower burden, and vice versa. CfDNA concentrations at baseline were measured and correlated to clinical outcome. The analysis revealed that a cfDNA concentration ≥0.7 ng/µL was predictive of a worse outcome (ROC curve). Specifically, in the 73 patients analyzed, those with cfDNA levels ≥0.7 ng/µL had a median PFS of 63.8 months compared to 88.5 months for patients with lower cfDNA levels (p=0.022). When examining the subset of 57 patients (biopsy sample available), the median PFS was 57.5 months vs 82.4 months (p=0.038). Additional details are available in the Supplementary Data.

Correlation of baseline ctDNA clonotype with clinical variables

The clonotype detection on ctDNA was correlated with pre-treatment clinical characteristics including histology, stage, lactate dehydrogenase (LDH), international prognostic index (IPI), B symptoms, extra nodal disease, and Eastern Cooperative Oncology Group Performance Status (ECOG PS). No statistically significant differences were found between ctDNA clonotype detection and histology, B symptoms, ECOG PS. In contrast, we recorded a significant association of clonality detection with IPI (intermediate/high) (p=0.02), elevated LDH (p=0.01, and stage (III/IV) (p=0.05). We found only a trend with the presence of extra nodal disease (p=0.11).

The 5 patients with no clonal marker detectable on ctDNA had favorable characteristics such as localized stage (80%, 4/5), low-risk IPI (100%, 5/5), absence of B symptoms (100%, 5/5), normal LDH (100%, 5/5) and absence of extra nodal disease (80%, 4/5). All are alive and in complete response (CR).

The 11 patients with a different clonal marker found on ctDNA compared to the tumor biopsy also had favorable characteristics, such as absence of B symptoms (100%, 11/11), ECOG PS 0-1 (100%, 11/11), normal LDH (72.7%, 8/11), low-risk/low-intermediate IPI (90.9%, 10/11). Among them, no relapse was observed. Additional details are available in the Supplementary Data and Supplementary Table S2.

Longitudinal monitoring of ctDNA MRD

The association between MRD and clinical data was assessed in 52 patients. Patients with discordant clonotype (11 cases) or absence of clonality on plasma (5 cases) or on biopsy (5 cases) were excluded (Supplementary Figure S1).

Longitudinal MRD analysis was performed on ctDNA samples during chemotherapy and at EOT. A total of 92 longitudinal plasma samples were studied: 45 at interim with two different time points (15 at C2D1, 30 at C4D1) and 47 at EOT, according to material availability.

The median plasma cfDNA concentration in the interim and EOT samples was 9.2 ng/mL (range 0.99-131) and 5.6 ng/mL (range 1.54-65.2), respectively.

ctDNA MRD during treatment

During treatment, ctDNA MRD analysis was possible in 45 patients: in 71.1% (32/45) the basal tumor clonotype disappeared and in 28.9% (13/45) it persisted. Interim MRD correlated significantly with PFS at the last follow-up, being 78.1% for MRD- *vs* 30.8% for MRD+ patients (p<0.0001), with an estimated median PFS of not reached (NR) *vs* 20.7 months (OR 1.97, range 1.1-3.5) (Figure 1A). The predictive power of interim MRD was confirmed at both time points (C2D1 p=0.001, C4D1 p=0.037). Additional details are available in the Supplementary Figure S2A-B.

Overall, among the 13 MRD+ patients, 9 (69.2%) progressed clinically, after 4.5-52 months from diagnosis, with 1 being refractory and 4 (30.8%) experiencing an early relapse. By contrast, only 7 of the 32 MRD- patients (21.9%) progressed after 16.6-48.5 months from diagnosis; none within 12 months.

Interim CT was available for 44/45 patients: 34.1% patients obtained a CR, 61.4% a partial response (PR) and 4.5% a stable/progressive disease (SD/PD).

Overall, the concordance between ctDNA MRD and radiological disease detected by interim CT was 52.3% (CR/MRD- or PR-SD-PD/MRD+). Interim ctDNA MRD could stratify the prognosis of the 27 patients in PR, as shown in Figure 1B, with a PFS of 78.9% for MRD- patients *vs* 37.5% for MRD+ patients (p=0.018). Only 4 PR patients showed undetectable ctDNA and subsequently relapsed, with an estimated median PFS of 57 months (range 32-61).

ctDNA MRD at EOT

At EOT, ctDNA MRD analysis was performed in 47 patients: 78.7% (37/47) were MRD- and 21.3% (10/47) were MRD+, with a PFS of 83.8% for MRD- patients *vs* 0% for MRD+ patients (p<0.0001) (Figure 2A). All 10 MRD+ patients relapsed, 3 (30%) within the first 12 months from diagnosis and 4 (40%) between 12 and 24 months. By contrast, only 6 of 37 MRD- patients (16.2%) progressed after 19.5-48.5 months from diagnosis; none within 12 months.

Overall, plasma ctDNA evaluation had no false positives at EOT, with a positive predictive value of 100%; indicating that all patients with a positive ctDNA test experienced disease progression. Conversely, the negative predictive value was 84%, reflecting that only 16% of patients with a negative ctDNA test experienced disease progression.

According to PET/CT disease assessment of final response, 85.1% patients (40/47) achieved a CR, 10.6% (5/47) had a PR/SD and 4.3% (2/47) showed a PD. A complete metabolic response at EOT was confirmed as a PFS predictor at univariate analysis (p=0.001). Overall, the concordance between ctDNA MRD and PET/CT was 72.3% (CR/MRD- or PR-SD-PD/MRD+).

A first subanalysis was performed in the 40 patients achieving a complete metabolic response by PET/CT; 8 (20%) were ctDNA MRD+ and all relapsed (0% *vs* 87.5%, p<0.0001), 2 experiencing an early relapse (Figure 2B). Only 1 PR patient was MRD+ by PET/CT and experienced a relapse.

A second subanalysis was performed to assess the impact of the kinetic of the detectable IG marker between interim time points and EOT in 42 patients in which MRD analysis was performed both during and after treatment: 61.9% (26/42) were double MRD- and 11.5% (3/26) experienced a relapse, 23.8% (10/42) were MRD+ at EOT and all relapsed irrespective of the interim MRD status; 14.3% (6/42) were MRD+ at interim evaluation and MRD- at EOT, and 33.3% (2/6) relapsed (p<0.0001, Figure 2C). In particular, 6 patients had double MRD+ at interim/EOT: 3 relapsed within 12 months (7.5, 9.9, 11.7, respectively), 1 at 15.4 months, 1 at 20.7 months and 1 at 52 months.

Multivariate analysis

Cox regression multivariate analysis (MVA) was performed combining all significant risk factors for PFS, which included: response at interim CT, response at EOT PET/CT, ctDNA MRD during treatment and ctDNA MRD at EOT. Interim MRD (HR 4.2; 95% CI, 1.3 to 13.4), metabolic response at EOT (HR 4.76; 95% CI, 1.3 to 17.3), and EOT MRD (HR 24.5; 95% CI, 5.9 to 100.8) were confirmed as independent prognostic factors, with the latter having the highest HR on PFS (p<0.0001).

OS analysis

At univariate analysis, ECOG PS 2-4 (p=0.05), response at interim CT (p=0.01), response at EOT PET/CT (p=0.05), ctDNA MRD during treatment (p=0.001) and ctDNA MRD at EOT (p<0.0001) were significant risk factors for OS and included in MVA. Interim MRD- patients presented at the last update an OS of 84.4%, compared to 38.5% for MRD+ patients (p<0.0001). MRD at EOT significantly predicted a worse OS in MRD+ patients (20%), compared to 86.5% for MRD- patients (p<0.0001). The estimated median OS was 32 months for MRD+ patients at interim time points and 30 months for those MRD+ at EOT, and not reached for the MRD negative patients at both time points. We performed a multivariate analysis that confirmed the predictive power of these parameters. MRD positivity at interim (HR 16.7; 95% CI, 1.7 to 160.1; p=0.014) and at EOT (HR 4.9; 95% CI, 1.1 to 20.6; p=0.02) and high ECOG PS (HR 14.9; 95% CI, 1.5 to 149.5; p=0.02) independently predicted a shorter OS.

DISCUSSION

Our retrospective observational study shows that in DLBCL patients the detection of a clonal marker and MRD analysis can be effectively applied to the plasma compartment (ctDNA) through an IG-based NGS approach. This method has been tested and validated on gDNA in other neoplasms, demonstrating high sensitivity and specificity for initial clonal characterization and disease monitoring compared to conventional methods.[29-32] At baseline, analysis of the IG gene rearrangements on the FFPE tissue biopsy and on pre-treatment plasma samples allowed to identify a clonal marker in 91.2% and 93.2% of patients, respectively. The utilization of all assay panels (FR1/2/3 and IGK) increased the detection rate of clonality in both compartments. Paired analysis of tumor tissue and plasma sample was possible in 52 cases showing consistent IG clonality in 36 (69.2%). In 5 cases, no clonality was found in ctDNA, suggesting limited disease spread, while a different clonal rearrangement was identified in 11 cases. Both subgroups had favorable clinical characteristics and outcome, indicating a potential clinical predictive value of the discordance. In 5 cases, a clonal marker was solely detected in the plasma compartment, and 2/5 patients relapsed; however, the absence of clonality in the tumor biopsy was attributed to low quality DNA, precluding further considerations. Consequently, these 21 cases were excluded from the MRD outcome analysis, the primary endpoint of this study. Overall, the total amount of cfDNA at baseline was predictive of PFS.

PET/CT is the recommended imaging strategy for treatment response assessment,[5,6] with the most accurate prognostic classification achieved by the EOT PET/CT.[33] Interim PET/CT conducted after two cycles of treatment has been explored for the early identification of chemo-refractory as well as good-risk patients, but it is not currently used in the clinical practice.[34,35] It is also known that

imaging techniques are limited by low sensitivity and/or specificity.[33-35] Our findings show that MRD analysis on ctDNA could overcome many of these limitations and refine the imaging-based evaluation of response, although nowadays a biopsy-proven relapse remains the gold standard.

MRD positivity at interim time points emerged as an independent prognostic factor especially in patients fulfilling Cheson's criteria of PR at interim CT (C2D1 $p<0.0001$, C4D1 $p=0.037$), indicating that an early MRD clearance during treatment is associated with a significantly favorable prognosis. These results align with other studies demonstrating that a decrease in ctDNA levels at early time points predicts a favorable outcome.[17-20]

At EOT, both MRD and PET/CT resulted independent predictors of PFS in multivariate analysis, but ctDNA MRD exhibited a higher predictive power (HR 24.5 positive MRD *vs* HR 4.76 for positive PET). MRD positivity predicted relapse in 67% of patients achieving a complete metabolic response, underscoring its relevance as a complement to PET/CT, with high specificity.

An increasing number of studies have explored MRD monitoring in DLBCL using IG-NGS or targeted-gene mutations approaches, all of which provided insights into patients' outcomes.[13] The first two studies based on IG ctDNA monitoring suggested that patients with undetectable IG rearrangement on ctDNA after two cycles of therapy had a longer PFS compared to ctDNA positive patients.[19,20] More recently, IG ctDNA MRD positivity in the apheretic stem cell collection of R/R DLBCL patients undergoing autologous transplantation was predictive of both PFS and OS.[21] Also in patients treated with CAR-T cells IG-MRD on ctDNA was predictive of clinical outcome,[22] and could help to clarify false PET-positive signals in the early assessment after infusion.[36] The latter studies[21,22,36] used the clonoSEQ IG-MRD NGS assay, commercially available and approved in the US to test bone marrow/PB in patients with multiple myeloma (MM), B-cell acute lymphoblastic leukemia (B-ALL) and chronic lymphocytic leukemia (CLL).

On the other hand, MRD monitoring by targeted-gene mutations in DLBCL was first evaluated by applying a CAPP-seq approach.[16,17] More recently, a CAPP-seq MRD monitoring on ctDNA has been used in the large Polarix trial, comparing R-CHOP versus polatuzumab-R-CHP at C5D1 and EOT.[37] Patients with undetectable MRD at both C5D1 and EOT showed a prolonged 3-year PFS and OS, irrespective of the treatment arm. Similar to our findings, ctDNA MRD refined the prognostic significance of the complete metabolic response at the EOT PET, but only in the experimental arm and not in the R-CHOP arm. A novel PhasED-seq approach has been proposed to overcome the low sensitivity of CAPP-Seq.[18,38] In Europe, the EuroClonality NGS DNA Capture (EuroClonality-NDC) assay, released to detect clonal IG and/or T-cell receptor gene rearrangements, translocations, copy-number alterations, and somatic mutations in lymphoproliferative disorders,[39] was applied to plasmatic ctDNA in DLBCL[40] with results mostly

in agreement with ours. A baseline molecular marker (either a single nucleotide variant, SNV, and/or translocation and/or clonal IG gene rearrangement) was identified from the plasma in 90% of 68 patients. As for other studies, pre-treatment ctDNA levels were significantly associated with known clinical parameters of tumor burden (LDH, stage and IPI).[10,17,22,40] In 19 cases with paired sequencing of lymphoma tissue, 19% of variants were only detected in tissue and 8% of SNVs were solely detected in ctDNA, mirroring, as in our study, the sensitivity limitation of ctDNA assay on the one hand and the theoretical advantage of ctDNA to capture spatial heterogeneity on the other hand. IG rearrangements resulted concordant between tissue and plasma in 84% of 19 cases. Both a quantitative 'major molecular response' (MMR), defined as a 2.5-log reduction in ctDNA after two treatment cycles, and a 'qualitative MMR', defined as the undetectable structural variants from plasma post-cycle two, were predictive of a prolonged PFS. Integrating MMR with interim PET refined PFS prediction. At variance from ours, in this paper[40] no EOT MRD evaluation was performed.

Finally, the concept of a dynamic measure of a given patient's risk throughout the course of the disease, based on serially collected longitudinal data, has gained increasing relevance for a superior outcome prediction.[41] Indeed, the CIRI (Continuous Individualized Risk Index) score is updated dynamically as additional information becomes available, such as MRD measure by ctDNA or interim imaging studies. The two-point MRD measure suggested by our paper and by others[37] supports the need of a dynamic evaluation of patients' prognosis.

Our results add to the literature testing in a real-life context of DLBCL another IG-NGS assay on ctDNA. Testing ctDNA is a feasible non-invasive and dynamic method that can be used as often as necessary to detect subclinical disease in longitudinally monitored tumor-related clones. We obtained the expected amount of cfDNA reported in the literature, with no samples excluded from the MRD analysis for insufficient quantity. However, the need of diagnostic tumor tissue still remains.

In the clinical setting, the possibility of MRD on ctDNA in identifying false negative CT or PET/CT results at interim time points and EOT, respectively, opens the scenario of pre-emptive immunotherapy strategies. Moreover, the early identification of poor responders to first-line therapy would enable the use of second-line CAR-T cells in patients with better clinical conditions and lower disease burden.

This study has some limitations: the relatively limited sample size, the lack of paired tumor tissue screening for all patients, the lack of an absolute quantification of MRD. Thus, more work needs to be done to optimize the proposed methodology and confirm its potential in larger series of patients. Moreover, comparative analyses are required across different ctDNA-MRD approaches in order to

identify the most suitable for clinical purposes. However, the detected IG clone in ctDNA proved positive at EOT in all R/R patients and negative in most of non-relapsing patients, indicating a homogenous clinical behavior of MRD+ and MRD- patients at EOT. This implies that despite the relatively low sensitivity, IG clone detection is clinically relevant and reflects the persistence of the disease.

The broad application of this and other testing modality in the routine practice is hindered by the lack of standardized guidelines. Indeed, despite the data provided in the literature in the last decade, we still face the absence of an established and standardized tool to monitor MRD in DLBCL on ctDNA, due to the uncertain balance between the optimal sensitivity and specificity and the lack of clinical and inter-laboratory validation of the different proposed approaches. Given the clinical relevance of this topic, the field is open to larger studies and coordinated efforts that aim at finally moving MRD monitoring in risk-adapted clinical trials and in the clinical practice of DLBCL patients.[42,43]

REFERENCES

1. Alaggio R, Amador C, Anagnostopoulos I, et al. The 5th edition of the World Health Organization classification of haematolymphoid tumours: lymphoid neoplasms. Leukemia. 2022;36(7):1720-1748.
2. Campo E, Jaffe ES, Cook JR, et al. The international consensus classification of mature lymphoid neoplasms: a report from the clinical advisory committee. Blood. 2022;140(11):1229-1253.
3. Sehn LH, Salles G. Diffuse large B-cell lymphoma. N Engl J Med. 2021;384(9):842-858.
4. Schmitz R, Wright GW, Huang DW, et al. Genetics and pathogenesis of diffuse large B-cell lymphoma. N Engl J Med. 2018;378(15):1396-1407.
5. Cheson BD, Fisher RI, Barrington SF, et al. Recommendations for initial evaluation, staging, and response assessment of Hodgkin and non-Hodgkin lymphoma: the Lugano classification. J Clin Oncol. 2014;32(27):3059-3068.
6. Crump M, Neelapu SS, Farooq U, et al. Outcomes in refractory diffuse large B-cell lymphoma: results from the international SCHOLAR-1 study. Blood. 2017;130(16):1800-1808.
7. Locke FL, Miklos DB, Jacobson CA, et al. Axicabtagene Ciloleucel as second-line therapy for large B-cell lymphoma. N Engl J Med. 2022;386(7):640-654.
8. Abramson JS, Solomon SR, Arnason J, et al. Lisocabtagene maraleucel as second-line therapy for large B-cell lymphoma: primary analysis of the phase 3 TRANSFORM study. Blood. 2023;141(14):1675-1684.
9. Roschewski M, Staudt LM, Wilson WH. Dynamic monitoring of circulating tumor DNA in non-Hodgkin lymphoma. Blood. 2016;127(25):3127-3132.
10. Scherer F, Kurtz DM, Newman AM, et al. Distinct biological subtypes and patterns of genome evolution in lymphoma revealed by circulating tumor DNA. Sci Transl Med. 2016;8(364):364ra155.
11. Rossi D, Spina V, Bruscaggin A, et al. Liquid biopsy in lymphoma. Haematologica. 2019;104(4):648-652.
12. Huet S, Salles G. Potential of circulating tumor DNA for the management of patients with lymphoma. JCO Oncol Pract. 2020;16(9):561-568.
13. Lauer EM, Mutter J, Scherer F. Circulating tumor DNA in B-cell lymphoma: technical advances, clinical applications, and perspectives for translational research. Leukemia. 2022;36(9):2151-2164.

14. Rivas-Delgado A, Nadeu F, Enjuanes A, et al. Mutational landscape and tumor burden assessed by cell-free DNA in diffuse large B-cell lymphoma in a population-based study. Clin Cancer Res. 2021;27(2):513-521.
15. Alig S, Macaulay CW, Kurtz DM, et al. Short diagnosis-to-treatment interval is associated with higher circulating tumor DNA levels in diffuse large B-cell lymphoma. J Clin Oncol. 2021;39(23):2605-2616.
16. Rossi D, Diop F, Spaccarotella E, et al. Diffuse large B-cell lymphoma genotyping on the liquid biopsy. Blood. 2017;129(14):1947-1957.
17. Kurtz DM, Scherer F, Jin MC, et al. Circulating tumor DNA measurements as early outcome predictors in diffuse large B-cell lymphoma. J Clin Oncol. 2018;36(28):2845-2853.
18. Meriranta L, Alkodsi A, Pasanen A, et al. Molecular features encoded in the ctDNA reveal heterogeneity and predict outcome in high-risk aggressive B-cell lymphoma. Blood. 2022;139(12):1863-1877.
19. Roschewski M, Dunleavy K, Pittaluga S, et al. Circulating tumour DNA and CT monitoring in patients with untreated diffuse large B-cell lymphoma: a correlative biomarker study. Lancet Oncol. 2015;16(5):541-549.
20. Kurtz DM, Green MR, Bratman SV, et al. Noninvasive monitoring of diffuse large B-cell lymphoma by immunoglobulin high-throughput sequencing. Blood. 2015;125(24):3679-3687.
21. Merryman RW, Redd RA, Taranto E, et al. Minimal residual disease in patients with diffuse large B-cell lymphoma undergoing autologous stem cell transplantation. Blood Adv. 2023;7(17):4748-4759.
22. Frank MJ, Hossain NM, Bukhari A, et al. Monitoring of circulating tumor DNA improves early relapse detection after axicabtagene ciloleucel infusion in large B-cell lymphoma: results of a prospective multi-institutional trial. J Clin Oncol. 2021;39(27):3034-3043.
23. Tilly H, Gomes da Silva M, Vitolo U, et al. Diffuse large B-cell lymphoma (DLBCL): ESMO clinical practice guidelines for diagnosis, treatment and follow-up. Ann Oncol. 2015;26(5_suppl):v116-v125.
24. Zelenetz AD, Gordon LI, Abramson JS, et al. NCCN guidelines insights: B-cell lymphomas, version 3.2019. J Natl Compr Canc Netw. 2019;17(6):650-661.
25. Cheson BD, Ansell S, Schwartz L, et al. Refinement of the Lugano classification lymphoma response criteria in the era of immunomodulatory therapy. Blood. 2016;128(21):2489-2496.
26. Soscia R, Della Starza I, De Novi LA, et al. Circulating cell-free DNA for target quantification in hematologic malignancies: Validation of a protocol to overcome pre-analytical biases. Hematol Oncol. 2023;41(1):50-60.

27. Shukla ND, Schroers-Martin JG, Sworder BJ, et al. Specificity of immunoglobulin high-throughput sequencing minimal residual disease monitoring in non-Hodgkin lymphomas. Blood Adv. 2024;8(3):780-784.
28. Højlund EL, Cédile O, Larsen TS, et al. Cell-free DNA for detection of clonal B cells in diffuse large B cell lymphoma by sequencing. Int J Lab Hematol. 2023;45(5):735-742.
29. Arcila ME, Yu W, Syed M, et al. Establishment of Immunoglobulin Heavy (IGH) Chain Clonality Testing by Next-Generation Sequencing for Routine Characterization of B-Cell and Plasma Cell Neoplasms. J Mol Diagn. 2019;21(2):330-342.
30. Ha J, Lee H, Shin S, et al. Ig Gene Clonality Analysis Using Next-Generation Sequencing for Improved Minimal Residual Disease Detection with Significant Prognostic Value in Multiple Myeloma Patients. J Mol Diagn. 2022;24(1):48-56.
31. Liu Y, Ho C, Yu W, et al. Quantification of Measurable Residual Disease Detection by Next-Generation Sequencing-Based Clonality Testing in B-Cell and Plasma Cell Neoplasms. J Mol Diagn. 2024;26(3):168-178.
32. Lay L, Stroup B, Payton JE. Validation and interpretation of IGH and TCR clonality testing by Ion Torrent S5 NGS for diagnosis and disease monitoring in B and T cell cancers. Pract Lab Med. 2020;22:e00191.
33. Adams HJ, Nievelstein RA, Kwee TC. Prognostic value of complete remission status at end-of-treatment FDG-PET in R-CHOP-treated diffuse large B-cell lymphoma: systematic review and meta-analysis. Br J Haematol. 2015;170(2):185-191.
34. Mamot C, Klingbiel D, Hitz F, et al. Final results of a prospective evaluation of the predictive value of interim positron emission tomography in patients with diffuse large B-cell lymphoma treated with R-CHOP-14 (SAKK 38/07). J Clin Oncol. 2015;33(23):2523-2529.
35. Schoder H, Polley MY, Knopp MV, et al. Prognostic value of interim FDG-PET in diffuse large cell lymphoma: results from the CALGB 50303 clinical trial. Blood. 2020;135(25):2224-2234.
36. Dean EA, Kimmel GJ, Frank MJ, et al. Circulating tumor DNA adds specificity to PET after axicabtagene ciloleucel in large B-cell lymphoma. Blood Adv. 2023;7(16):4608-4618.
37. Herrera AF, Tracy S, Sehn LH, Jardin F. Circulating tumor DNA (ctDNA) status and clinical outcomes in patients (pts) with previously untreated diffuse large B-cell lymphoma (DLBCL) in the Polarix study. J Clin Oncol. 2023;41(16_suppl):7523.
38. Kurtz DM, Soo J, Co Ting Keh L, et al. Enhanced detection of minimal residual disease by targeted sequencing of phased variants in circulating tumor DNA. Nat Biotechnol. 2021;39(12):1537-1547.

39. Stewart JP, Gazdova J, Darzentas N, et al. Validation of the EuroClonality-NGS DNA capture panel as an integrated genomic tool for lymphoproliferative disorders. Blood Adv. 2021;5(16):3188-3198.
40. Alcoceba M, Stewart JP, García-Álvarez M, et al. Liquid biopsy for molecular characterization of diffuse large B-cell lymphoma and early assessment of minimal residual disease. Br J Haematol. 2024;205(1):109-121.
41. Kurtz DM, Esfahani MS, Scherer F, et al. Dynamic Risk Profiling Using Serial Tumor Biomarkers for Personalized Outcome Prediction. Cell. 2019;178(3):699-713.e19
42. Poynton E, Okosun J. Liquid biopsy in lymphoma: is it primed for clinical translation? EJHaem. 2021;2(3):616-627.
43. Pirosa MC, Borchmann S, Jardin F, Gaidano G, Rossi D. Controversies in the Interpretation of Liquid Biopsy Data in Lymphoma. Hemasphere. 2022;6(6):e727.

Table 1A. Patients' characteristics

		Rome cohort (n = 41)	Novara cohort (n = 32)	Entire cohort (n = 73)	*p*
Sex	Male	24 (58.5)	14 (43.8)	38 (52.1)	0.2
	Female	17 (41.5)	18 (56.3)	35 (47.9)	
Diagnosis	DLBCL, NOS	27 (65.9)	22 (68.8)	49 (67.1)	0.9
	HGBCL with rearrangements*	5 (12.2)	5 (15.7)	10 (13.7)	
	Transformations of iBCL	5 (12.2)	3 (9.4)	8 (11.0)	
	HGBCL, NOS	4 (9.8)	2 (6.3)	6 (8.2)	
Age	Median years (range)	63.9 (26.2-78.6)	69 (19-85)	65.19 (19-85)	0.12
Age	<65 years	23 (56.1)	12 (37.5)	35 (47.9)	0.11
	≥65 years	18 (43.9)	20 (62.5)	38 (52.1)	
Extra nodal disease	No	19 (46.3)	8 (25.0)	27 (37.0)	0.07
	Yes	22 (53.7)	24 (75.0)	46 (63.0)	
B symptoms	No	33 (80.5)	25 (78.1)	58 (79.5)	0.8
	Yes	8 (19.5)	7 (21.9)	15 (20.5)	
Elevated LDH	Yes	18 (43.9)	20 (62.5)	38 (52.1)	0.11
	No	23 (56.1)	12 (37.5)	35 (47.9)	
ECOG PS	0-1	35 (85.4)	29 (90.6)	64 (87.7)	0.49
	2-4	6 (14.6)	3 (9.4)	9 (12.3)	
IPI risk	Low	18 (43.9)	10 (31.3)	28 (38.4)	0.68
	Low-intermediate	7 (17.1)	7 (21.9)	14 (19.2)	
	High-intermediate	6 (14.6)	7 (21.9)	13 (17.8)	
	High	10 (24.4)	8 (25.0)	18 (24.7)	
Stage	I-II	19 (46.3)	13 (40.6)	32 (43.8)	0.62
	III-IV	22 (53.7)	19 (59.4)	41 (56.2)	
Treatment plan	R-CHOP-21	34 (82.9)	23 (71.9)	57 (78.1)	0.42
	Lower intensity than R-CHOP-21°	2 (4.9)	4 (12.5)	6 (8.2)	
	Higher intensity than R-CHOP-21#	5 (12.2)	5 (15.6)	10 (13.7)	
Follow-up	Median months (range)	39.02 (5-63.07)	42.5 (1.47-72.3)	39.1 (1.47-72.3)	0.78
Clonal marker on tumor biopsy	No	2 (6.5)	3 (11.5)	5 (8.8)	0.49
	Yes	29 (93.5)	23 (88.5)	52 (91.2)	
Clonal marker on ctDNA	No	3 (7.3)	2 (6.3)	5 (6.8)	0.97
	Different from tumor biopsy	6 (14.6)	5 (15.6)	11 (15.1)	
	Yes	32 (78.0)	25 (78.1)	57 (78.1)	

NOTE: Data presented as No. (%) unless otherwise indicated.
*rearrangements of MYC and/or BCL2 and/or BCL6
°R-CHOP-like regimen with lower intensity: R-mini-CHOP/COMP. # Higher intensity: R-CHOP14-CODOX/M-IVAC.
13 patients received radiotherapy (plasma samples were collected at the end of chemoimmunotherapy, before radiotherapy).
Abbreviations: DLBCL, diffuse large B-cell lymphoma; NOS, not otherwise specified iBCL, indolent B-cell lymphoma; HGBCL, high grade B-cell lymphoma; LDH, lactate dehydrogenase; ECOG PS, Eastern Cooperative Oncology Group performance status; IPI, international prognostic index; R-CHOP, rituximab plus cyclophosphamide, doxorubicin, vincristine, and prednisone; ctDNA, circulating tumor DNA.

Table 1B. Patients' outcome

		Rome cohort	Novara cohort	Entire cohort	*p*
Response at interim (Cheson Criteria)	CR	19 (47.5)	7 (25.0)	26 (38.2)	0.14
	PR	20 (50.0)	19 (67.9)	39 (57.4)	
	SD/PD	1 (2.5)	2 (7.1)	3 (4.4)	
MRD at interim time points	Negative	29 (72.5)	14 (77.8)	43 (74.1)	0.67
	Positive	11 (27.5)	4 (22.2)	15 (25.9)	
MRD at EOT	Negative	31 (79.5)	23 (88.5)	54 (83.1)	0.34
	Positive	8 (20.5)	3 (11.5)	11 (16.9)	
Response at EOT by PET/CT	CR	35 (85.4)	29 (90.6)	64 (87.7)	0.56
	PR/SD	4 (9.8)	1 (3.1)	5 (6.8)	
	PD	2 (4.9)	2 (6.3)	4 (5.5)	
CR	CR	35 (85.4)	29 (90.6)	64 (87.7)	0.49
	No CR	6 (14.6)	3 (9.4)	9 (12.3)	
R/R disease	No progressive disease	28 (68.3)	25 (78.1)	53 (72.6)	0.35
	R/R after first line	13 (31.7)	7 (21.9)	20 (27.4)	
Status at follow-up	Alive	30 (73.2)	26 (81.3)	56 (76.7)	0.41
	Dead	11 (26.8)	6 (18.8)	17 (23.3)	

NOTE: Data presented as No. (%) unless otherwise indicated. Full count is not available for all variables due to lack of data.
Abbreviations: CR, complete response; PR, partial response; SD/PD, stable/progressive disease; MRD, minimal residual disease; EOT, end of treatment; PET/CT, positron emission tomography/computed tomography; R/R, relapsed/refractory.

Figure Legends

Legend to Figure 1

Prognostic value of molecular measurable residual disease (MRD) on circulating tumor DNA (ctDNA) during treatment. (A) Kaplan-Meier estimates of progression-free survival (PFS) from diagnosis for patients evaluated at interim time points stratified by MRD positivity or negativity are shown. (B) Kaplan-Meier estimates show the PFS of patients in partial response (PR) at the interim computed tomography (CT) scan stratified by ctDNA MRD status.

Legend to Figure 2

Prognostic value of molecular measurable residual disease (MRD) on circulating tumor DNA (ctDNA) at the end of treatment (EOT). (A) Kaplan-Meier estimates of progression-free survival (PFS) from diagnosis for patients evaluated at EOT stratified by MRD status (positive or negative) are shown. (B) Kaplan-Meier estimates show the impact of MRD status on PFS in patients achieving final complete metabolic response according to positron emission tomography/computed tomography (PET/CT). (C) Kaplan-Meier estimates show the PFS of patients based on the combination of MRD status during and after treatment. Patients are categorized into four groups: double negative MRD (-/-), double positive MRD (+/+), MRD positive during treatment and MRD negative at EOT (+/-), MRD negative during treatment and MRD positive at EOT (-/+).

A Progression-free survival (months) all patients (N=45)

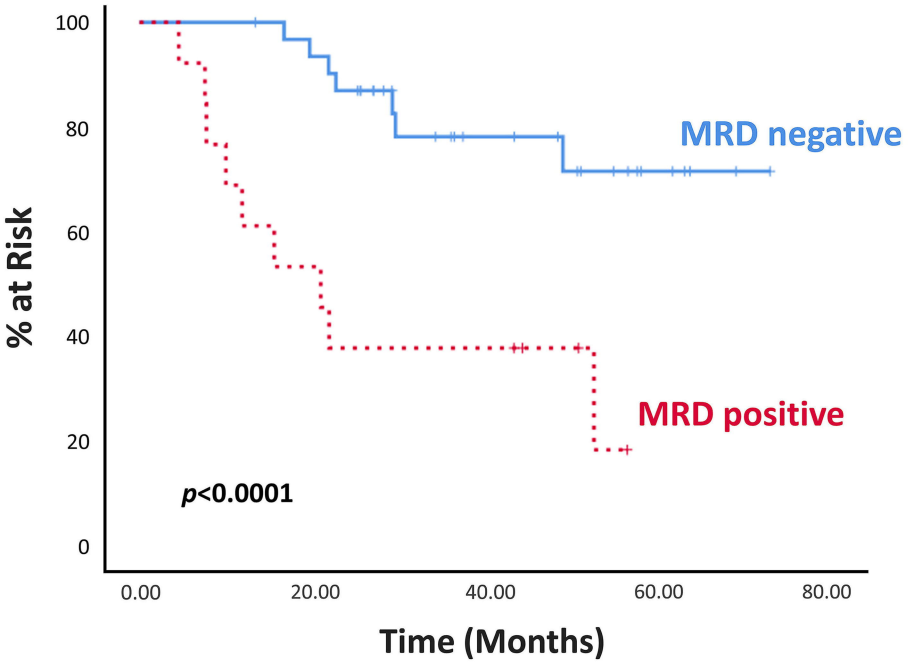

No. at risk:

MRD -	32	29	14	5	0
MRD +	13	7	5	0	0

B Progression-free survival (months) PR patients (N=27)

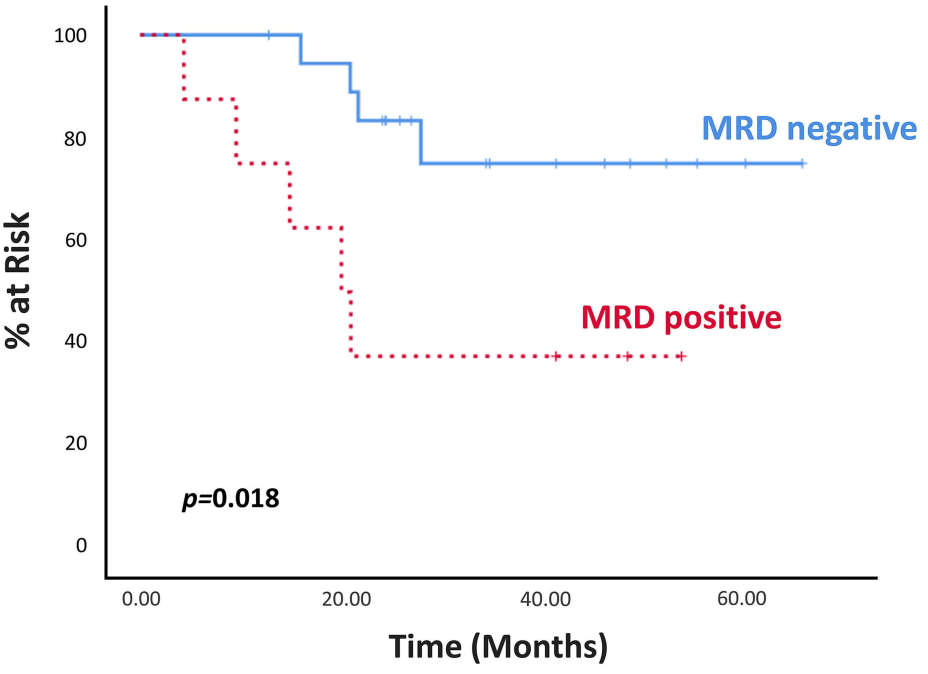

No. at risk:

MRD -	19	17	7	2
MRD +	8	5	3	0

A

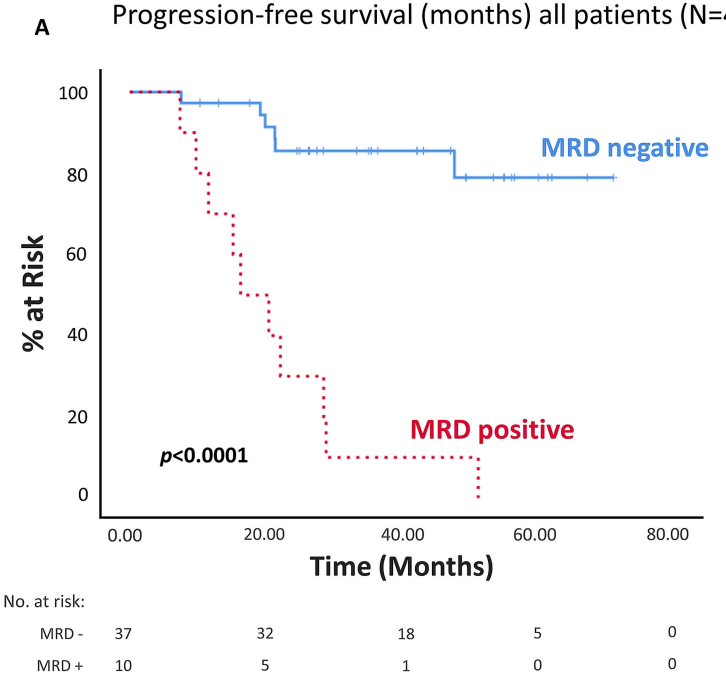

No. at risk:

MRD -	37	32	18	5	0
MRD +	10	5	1	0	0

B

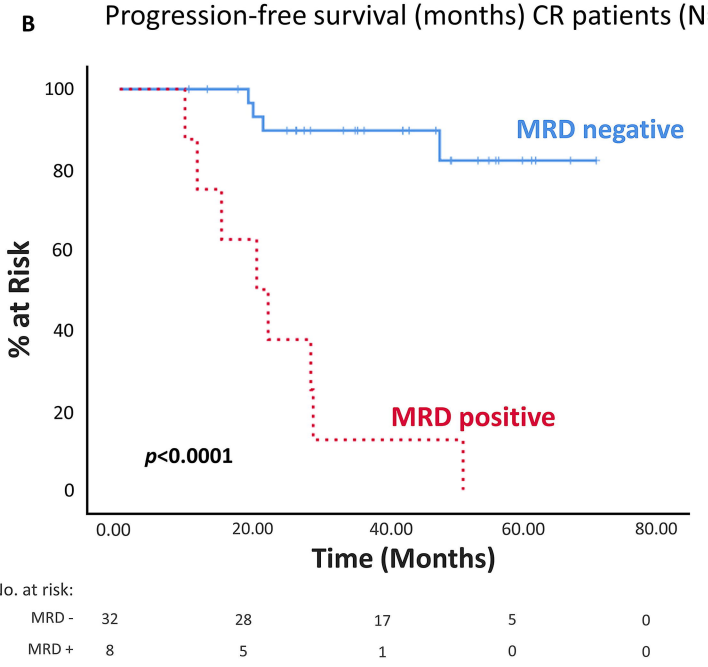

No. at risk:

MRD -	32	28	17	5	0
MRD +	8	5	1	0	0

C

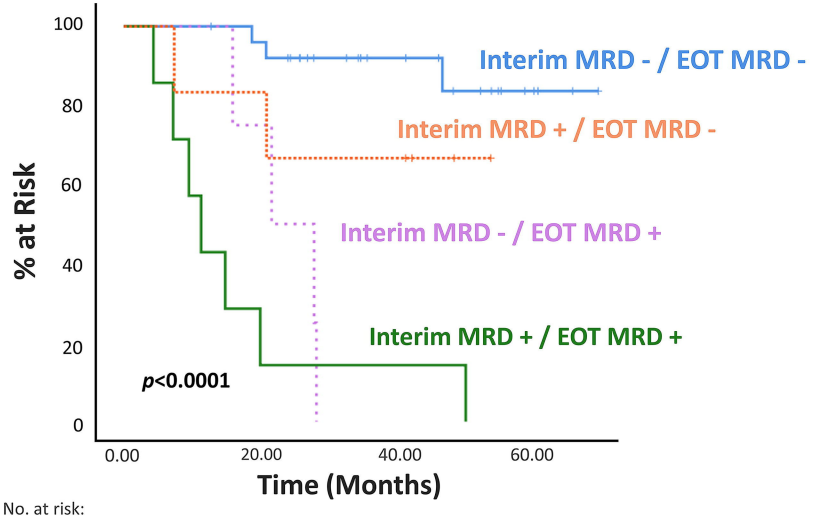

No. at risk:

MRD - / -	26	24	13	5
MRD - / +	4	3	0	0
MRD + / +	6	2	1	0
MRD + / -	6	5	4	0

Supplementary Data

Molecular measurable residual disease by immunoglobulin gene rearrangements on circulating tumor DNA predicts outcome in diffuse large B-cell lymphoma

SUPPLEMENTARY METHODS

Plasma cfDNA extraction

Peripheral blood (30 ml) was collected in EDTA tubes (Becton Dickinson, Franklin Lakes, NJ), since plasma processing was performed promptly, with separation completed within 4 hours at +4 °C. Tubes were centrifuged at 800 g for 10 min using a refrigerated centrifuge to separate plasma from cells. Plasma was then removed into new 1.5 ml tubes without disturbing the buffy coat and further centrifuged at 13,000 rpm for 10 min using a refrigerated centrifuge to remove any remaining cells. Plasma was stored in 1 ml aliquots at -80°C until DNA extraction. A rapid processing of blood samples soon after the venipuncture avoided cfDNA contamination from gDNA that may occur due to nucleated cell lysis and allowed to avoid dedicated tubes.

cfDNA was extracted from a total of 4 ml aliquots of plasma immediately after thawing by using the Maxwell RSC LV ccfDNA kit (Promega) and quantified by using the Qubit Fluorometer 3.0 (Thermo Fisher). cfDNA purity (as referred to absence of gDNA contamination) was established by capillary electrophoresis using an Agilent 2100 Bioanalyzer (Agilent Technologies Inc., Santa Clara, CA) equipped with the Expert 2100 software, in combination with a high sensitivity (HS) DNA microchip and HS DNA kit (Agilent Technologies). The assay was performed according to the instructions provided by the manufacturer.

NGS for clonality assessment and MRD analysis

Each LymphoTrack assay panel has a single multiplex master mix that targets conserved regions in the IGH or IGK genes. The LymphoTrack IGH FR1/2/3 assay panel uses primers targeting the IG framework regions (FR) to amplify V(D)J rearrangements. Each single FR multiplex master mix for IGH contains forward primers targeting one of the conserved framework regions (FR1, FR2, or FR3), as well as several consensus reverse primers targeting the JH region. Targeting all three framework regions significantly reduces the risk of not detecting the presence of clonality, as somatic hypermutations in the primer binding sites of the involved VH gene segments can impede DNA amplification.

On cfDNA samples, FR1 multiplex master mixes were excluded due to the small fragment size of cfDNA of ~166 bp.

The LymphoTrack IGK assay panel contains forward primers targeting the conserved VK region and intron sequences, with reverse primers targeting the JK and KDE regions. In 1-step PCR amplicons are generated and indexed, allowing the simultaneous sequencing of up to 24 samples in a single run. Each of these 24 indices can be considered to act as a unique barcode that allows amplicons from

individual samples to be pooled together after PCR amplification to generate the sequencing library. All baseline samples were sequenced using 150 ng of gDNA. Positive and negative controls for clonality were also included. Amplicons purity and quantity were assessed using the KAPA Library Quantification Kits for Illumina platforms (KAPA Biosystems, Boston, MA). Calculating the concentration of PCR amplicons allowed equal amplicon representation in the final pooled library. After demultiplexing, bioinformatics analysis was done by processing FASTQ files, generated during NGS, with the LymphoTrack Software-MiSeq v2.4.3 (Invivoscribe) to retrieve sequences from virtually every clonal B cell in the samples. Tumor associated clones at diagnosis were identified following three criteria: (1) 20,000 or more total reads for each sample; (2) at least 1, but not more than 2, merged top reads with 2.5% or greater (for IGH) and 5.0% or greater (for IGK) of total reads; and (3) top first or second merged reads at least two times more abundant than the third most abundant read to be considered clonotypic (for IGH), top first or second merged reads at least two times more abundant than the fifth most frequent merged sequence if there is at least ore INTR-Kde rearrangement detected in the four most frequent merged sequences or the third if there are no INTR-Kde detected (for IGK). The result of each assay was called as clonal, non-clonal or indeterminate (i.e., too few reads for evaluation). Data from the run were considered invalid if either the % cluster passing filter or the % base calls above Q30 were below 75%.

The same assay panels were used to assess MRD following similar methods as described above. Testing was done using only the primer sets that successfully characterized the diagnostic clone. To maximize the probability of detecting clonality in cfDNA samples, testing was conducted in triplicate reactions utilizing the maximum amount of cfDNA allowed by the protocol (10 µl). Each run included a no-template control and a low positive control (LPC, MRD level = 1E-04). However, a spike-in for MRD level quantification was omitted to prioritize the detection of clonal sequences in ctDNA, maximizing read numbers. Multiplexed libraries were sequenced using 500-bp paired-end runs on a MiSeq sequencer (Illumina). The FASTQ files were analyzed using the LymphoTrack Software-MiSeq v2.4.3 (Invivoscribe), and MRD analysis was performed with the bioinformatics LymphoTrack MRD Software v2.0.2 (Invivoscribe) tool considering the number of replicates, the amount of DNA (ng) for each replicate, the "Unique Reads" file generated with the LymphoTrack Software-MiSeq v2.4.3 (Invivoscribe) and the number of total reads. The MRD Software generates an "output.tsv" file with the full analysis of each sequence and a PDF report with the MRD results for each PCR replicate analyzed. For a "MRD Detected" result, the software reports the number of reads and cumulative frequencies of exact matched sequences and similar sequences (up to two mismatched nucleotides). For a "MRD Not Detected" result, the software reports the number of reads and cumulative frequencies of exact matched sequence and similar sequences (up to two mismatched

nucleotides). The detection limit and the relative % confidence of each MRD experiment was calculated on the basis of the number of replicates, the amount of DNA (ng) for each replicate, and the number of total reads.

Sequencing results were considered invalid when fewer than 20.000 total reads were retrieved.

Limit of detection of IGH and IGK assays on plasma

The limit of detection (LOD) of the LymphoTrack IGH and IGK assays on plasma was evaluated by analyzing the 23 positive MRD samples.

For each sample, the total number of reads of the clonotype sequence for all replicates (allowing up to 2 mismatch) was divided by the total number of sequencing reads generated for that sample and expressed as a percentage. This percentage was then multiplied by the amount of input cfDNA (expressed as ng) loaded for all PCR replicates, resulting in the Cumulative Target Read Count ($CTRC_{sample}$). The same calculation was performed for the LPC, which was included in each MRD experiment ($CTRC_{LPC}$). To estimate the expected read frequency for each sample, the $CTRC_{sample}$ and $CTRC_{LPC}$ values were related through a proportion, assuming that the LPC corresponds to an average expected read frequency of 0.0001, as per the application guide.

The formula used was:

$X_{sample} = 0.0001 \times CTRC_{sample} / CTRC_{LPC}$

where X_{sample} represents the expected read frequency of the sample.

Thus, a read frequency detection gradient was defined, relative to the percentage of target reads identified compared to a standard. The MRD experiments showed a $LOD_{maximum}$ of 5.3E-05 and a $LOD_{reproducible}$ of 6.3E-04.

Comparative Analysis of NGS and PCR/ddPCR in MRD Sample Detection

A comparative analysis between NGS and PCR/ddPCR was conducted on 8 MRD samples (4 at interim and 4 at EOT). Two of these samples were analyzed using both ddPCR and NGS, with results showing 100% concordance for both positive and negative detections. Due to the insufficient sensitivity and specificity of the derived allele-specific primers, the remaining 6 samples were analysed using conventional PCR and NGS. Among these 6 samples, a 67% concordance rate (4/6 samples) was observed between the methods: 2 samples resulted MRD positive by PCR and negative by NGS.

Statistical analysis

A ROC curve was employed to determine a cut-off for continuous variables.

SUPPLEMENTARY RESULTS

IG analysis of gDNA from FFPE

Compared with the reference germline sequence, most IG clones showed high somatic hypermutation rates, with a median rate of 7.4% (range 0.0% to 35.8%).

Pre-treatment ctDNA IG analysis

The clonal IG rearrangements identified in ctDNA were matched with the lymphoma-specific clonotype. Most cases had clonal rearrangements identified by the same assay (67.3%, 35/52), in 10 cases (19.2%, 10/52) a slight difference in the assay was observed (5 tumor biopsies were characterized by all three IGH assays and only by one or two IGH assays on ctDNA, and 5 biopsies were characterized by IGH-FR2/3 and only by one IGH assay on ctDNA), in the remaining 7/52 samples (13.5%) a different clonality characterized the two compartments (n=2) or no clonality was identified on ctDNA (n=5).

Correlations of baseline cfDNA levels with outcome and clonality

CfDNA concentrations at baseline were measured and correlated to clinical outcome, as reported in the results. CfDNA concentrations were also correlated with the presence or absence of clonality in the plasma. Cases with different clonal markers between the tumor biopsy and plasma were also examined. The rate of clonality detection on pre-treatment ctDNA correlated with the relative concentrations of cfDNA. The optimal cut-off for cfDNA concentration was 0.6 ng/µL (p=0.027, OR 2.35, range 1.17-4.79).

Discordant cases

In 11/52 (21%) patients with a different clonality identified in each compartment (diagnostic FFPE tissue and cfDNA), further analyses were conducted to enhance the characterization of these cases. The median amount of cfDNA was 0.692 ng/µL (range 0.27-4.73).

As a first step, the tumor biopsy site was evaluated (whether lymph node or extra nodal site). Out of the 11 patients, 6 biopsies were derived from extra-nodal tissue and 5 from lymph nodes. Therefore, there was no significant difference in the site of biopsy that could justify a discordant clonality. Additionally, 8 out of the 11 patients were studied through a mutation analysis approach. The LyV4.0 CAncer Personalized Profiling by deep Sequencing Assay (CAPP-seq) was utilized and conducted at the Novara center. A targeted resequencing gene panel, including coding exons and splice sites of 59 genes that are recurrently mutated in DLBCL and in other B cell malignancies, has been specifically

designed. Mutational analysis revealed somatic non-synonymous mutations in 100% (8/8) of tumor biopsies and 75% (6/8) of ctDNA samples, with notable heterogeneity across compartments in some patients. In certain cases, distinct mutations were detected in ctDNA compared to tumor biopsies, underscoring potential compartmental difference. See Supplementary Table S3.

In 2 out of 8 patients, different mutated genes were detected in the ctDNA and tumor biopsy, mirroring our findings on IG-NGS clonality. In 2 further patients several mutations were identified only in the biopsied tumor tissue, with no mutations found in the ctDNA. For 2 other patients, only one mutated gene was detected in the ctDNA, and the identical mutation was present in the tumor biopsy, alongside with additional mutations exclusively detected in the biopsy. In the remaining 2 patients, the same mutated genes were identified both in the ctDNA and tumor biopsy but represented only a fraction of the mutations identified in the latter.

Therefore, gene mutations analysis also reveals a heterogeneity across compartments in these patients, although differences in the IG-NGS and CAPP-Seq assays does not allow to drive further conclusions.

Plasma IG analysis of healthy donors

The cfDNA of 7 healthy donors was analyzed with the IGH (FR2/FR3) and IGK assay panels and subjected to identical analysis as the patients' pre-treatment samples. The median plasma cfDNA concentration was 4.2 ng/mL (range 2.7-7.8). Clonality was detected in 1/7 donors using both FR2 and FR3 assays. In 4/7 donors, clonality was detected, albeit with a "borderline" percentage of total reads: in 3/4 only with the FR2 assay and in 1/4 only with the FR3 assay. The remaining 2/7 donors exhibited a polyclonal pattern. The expansion of these minor clones in the plasma of healthy donors does not imply the presence of a malignancy, rather parallels what seen in the background amplification of the RQ-PCR assay, that is the non-specific amplification of comparable IG gene rearrangements presents in normal cells.

MRD positivity frequency according to the type of rearrangement

Among the patients who underwent MRD analysis on plasma samples, 27 were found suitable for monitoring with the FR3, 20 with the FR2 and 12 with the IGK rearrangement. The frequency of MRD positivity was then analyzed in relation to the type of rearrangement tracked in plasma. Among 53 samples analyzed by FR3, 15 were positive (28.3%); for the 35 samples analyzed by FR2, 8 were positive (22.9%), with no significant difference (p=0.63). Out of 18 samples analyzed by IGK, 2 were positive (11.1%). The lower number of tests with IGK is attributed to the limited number of patients monitored with this rearrangement.

Supplementary Table S1. This table presents the results of IGH and IGK gene rearrangements identified through NGS analysis conducted as part of this study.

N.	Assay on tumor biopsy	Clone 1	Clone 2	Assay on ctDNA	Clone 1	Clone 2
1	IGK	V2-30*01-J2*04		IGK	V2-30*01-J2*04	
2	IGK	V4-1*01-J3*01		IGK	V4-1*01-J3*01	
3	FR1+FR2+FR3	V3-30-5*02-J6*02	V3-30-5*02-J6*02	FR3	V3-30-5*02-J6*02	V3-30-5*02-J6*02
4	FR3	V4-34*13-J4*02	V4-61*07-J4*02	FR3	V4-34*13-J4*02	V4-61*07-J4*02
5	FR2+FR3	V3-35*01-J3*02		FR2+FR3	V3-35*01-J3*02	
6	FR3	V3-72*01-J5*02		FR3	V3-72*01-J5*02	
7	IGK	V4-1*01-J2*01		IGK	V4-1*01-J2*01	
8	FR1+FR2+FR3	V3-21*02-J4*02		FR2	V3-21*02-J4*02	
9	FR2	V1-8*01-J6*02		FR2	V1-8*01-J6*02	
10	FR1+FR2+FR3	V4-34*02-J4*02		FR3	V4-34*02-J4*02	
11	FR2	V2-5*08-J4*02		FR2	V2-5*08-J4*02	
12	FR2	V3-33*06-J4*02		FR2	V3-33*06-J4*02	
13	FR2+FR3	V3-48*03-J4*02		FR2+FR3	V3-48*03-J4*02	
14	FR2+FR3	V4-39*02-J6*02		FR2+FR3	V4-39*02-J6*02	
15	FR1+FR2+FR3	V1-46*01-J6*02	V4-28*01-J6*02	FR2+FR3	V1-46*01-J6*02	V4-28*01-J6*02
16	FR2	V3-64*04-J3*02		FR2	V3-64*04-J3*02	
17	FR3	V3-49*05-J4*02		FR3	V3-49*05-J4*02	
18	FR2+FR3	V1-2*03-J4*02		FR2+FR3	V1-2*03-J4*02	
19	FR2	V1-46*02-J4*02		FR2	V1-46*02-J4*02	
20	FR3	V1*01-J4*02		FR3	V1*01-J4*02	
21	FR2+FR3	V4-34*02-J4*02		FR3	V4-34*02-J4*02	
22	FR2+FR3	V1-46*02-J4*02		FR2	V1-46*02-J4*02	
23	FR3	V1-1*01-J4*02		FR3	V1-1*01-J4*02	
24	FR3	V2-70*11-J4*02		FR3	V2-70*11-J4*02	
25	FR2+FR3	V3-48*03-J4*02		FR2+FR3	V3-48*03-J4*02	
26	IGK	INTR-Kde		IGK	INTR-Kde	
27	IGK	V2-30*01-J5*01		IGK	V2-30*01-J5*01	
28	IGK	V2-24*01-J4*01		IGK	V2-24*01-J4*01	
29	IGK	V2-29*01-J5*01	V1-27*01-J5*01	IGK	V2-29*01-J5*01	V1-27*01-J5*01
30	FR2	V3-74*03-J4*02		FR2	V3-74*03-J4*02	
31	IGK	V2-29*03-J4*01		IGK	V2-29*03-J4*01	
32	FR2+FR3	V4-34*12-J5*02		FR2+FR3	V4-34*12-J5*02	
33	IGK	V4-1*01-J4*01		IGK	V4-1*01-J4*01	
34	FR2	V5-51*04-J5*02		FR2	V5-51*04-J5*02	
35	FR2	V1-2*04-J5*02		FR2	V1-2*04-J5*02	
36	FR2	V4-59*05-J3*01		FR2	V4-59*05-J3*01	
37	FR1+FR2+FR3	V4-34*13-J3*01		FR2+FR3	V2-5*02-J4*02	
38	FR2+FR3	V4-61*08-J6*02		FR3	V3-23*01-J4*02	
39	FR1	V3-30-3*02-J1*01	V3-30-3*02-J1*01	FR2	V3-15*01-J3*01	
40	IGK	V3-15*01-J4*01		IGK	V5-2*01-J1*01	V3-7*04-J4*01
41	IGK	INTR-Kde		IGK	V2-28*01-Kde	
42	FR2	V3-9*01-J5*02	V3-30*18-J4*02	FR2	V3-23*04-J6*03	V1-2*03-J4*02

43	FR2	V4-59*08-J3*02	V3-30-3*01-J4*02	FR3	V2-5*01-J5*02
44	FR3	V1-46*01-J6*02		FR3	V1-3*01-J4*02
45	FR2+FR3	V3-30*18-J4*02		FR3	V1-18*01-J3*02
46	FR3	V4-59*10-J3*02	V5-51*02-J4*02	FR3	V1-3*04-J6*02
47	FR2+FR3	V4-34*13-J4*02		FR3	V4-28*06-J6*02
48	FR3	V1-2*04-J6*02		-	
49	FR3	V1-46*01-J4*02		-	
50	FR1+FR2	V3-66*02-J6*02		-	
51	FR2+FR3	V4-34*01-J6*03		-	
52	FR2	V3-49*02-J6*03	V3-49*02-J6*03	-	

The 36 cases with concordant IG rearrangements are highlighted in bold.
Abbreviations: ctDNA, circulating tumor DNA; IGK, immunoglobulin kappa light chain gene rearrangement; FR, framework region.

Supplementary Table S2. This table presents the comparison of baseline clinical characteristics among three groups of patients categorized based on their clonality status.

		Group A	Group B	Group C	*p*
Age	<65y	4 (80.0)	7 (63.6)	21 (40.4)	.14 [a]
	≥65y	1 (20.0)	4 (36.4)	31 (59.6)	.18 [b]
Stage	I-II	4 (80.0)	6 (54.5)	20 (38.5)	.15 [a]
	III-IV	1 (20.0)	5 (45.5)	32 (61.5)	.32[b]
IPI risk	Low	5 (100.0)	7 (63.6)	15 (28.8)	
	Low-intermediate	0 (0.0)	3 (27.3)	9 (17.3)	.012[a]
	High-intermediate	0 (0.0)	0 (0.0)	11 (21.2)	.05[b]
	High	0 (0.0)	1 (9.1)	17 (32.7)	
ECOG PS	0-1	5 (100.0)	11 (100.0)	43 (82.7)	.23[a]
	2-4	0 (0.0)	0 (0.0)	9 (17.3)	.15[b]
B symptoms	No	5 (100.0)	11 (100.0)	39 (75)	.07[a]
	Yes	0 (0.0)	0 (0.0)	13 (25)	.05[b]
Extra nodal disease	No	4 (80.0)	3 (27.3)	18 (34.6)	.1[a]
	Yes	1 (20.0)	8 (72.7)	34 (65.4)	.6[b]
Elevated LDH	Yes	0 (0.0)	3 (27.3)	32 (61.5)	.006[a]
	No	5 (100.0)	8 (72.7)	20 (38.5)	.03[b]

NOTE: Data presented as No. (%) unless otherwise indicated.

These analyses consider the comparison of baseline clinical characteristics among three groups of patients. (**Group A**) Patients with undetectable clonality on plasma ctDNA at baseline. (**Group B**) Patients with detectable clonality on plasma ctDNA at baseline but different from the clonality assessed on the tumor biopsy. (**Group C**) Patients with the same clonality detected on both plasma ctDNA and tumor biopsy at baseline.

[a] refers to univariate analysis of patients with undetectable clonality on ctDNA

[b] refers to univariate analysis of patients with a different clonality between ctDNA and tumor biopsy

Abbreviations: ctDNA, circulating tumor DNA; IPI, international prognostic index; ECOG PS, Eastern Cooperative Oncology Group performance status; LDH, lactate dehydrogenase.

Supplementary Table S3. Gene mutations identified by CAPP-seq in 8 of the discordant cases. The specific gene mutations with variant allele frequency (VAF) and number of reads are shown in detail.

Sample ID	Gene	Nucleotide Change	AA Change	VAF Tumor	READS Tumor	VAF Plasma	READS Plasma
3	ACTB	c.241G>A	p.D81N	11.75%	78/664	9.12%	33/362
	CREBBP	c.3233C>A	p.S1078*	5.33%	44/826	12.73%	280/2199
	CREBBP	c.4849C>A	p.L1617M	-	-	0.83%	23/2784
	HIST1H1E	c.319C>T	p.L107F	-	-	1.93%	66/3416
	HIST1H2BK	c.31C>T	p.P11S	8.22%	496/6034	5.99%	74/1236
	KMT2D	c.11069delG	p.G3690fs*59	-	-	0.73%	18/2467
	PIM1	c.449C>A	p.S150Y	5.78%	160/2766	3.28%	51/1554
	PIM1	c.475C>T	p.H159Y	6.18%	144/2331	3.46%	62/1793
	PIM1	c.710G>A	p.S237N	7.31%	388/5305	2.53%	47/1858
	PIM1	c.847C>G	p.L283V	5.21%	622/11934	3.57%	56/1568
	PIM1	c.334C>T	p.H112Y	-	-	4.89%	48/982
	PIM1	c.384G>T	p.Q128H	-	-	5.04%	75/1489
	PIM1	c.511C>A	p.L171M	-	-	2.89%	51/1767
	PIM1	c.823C>T	p.L275F	-	-	3.09%	52/1681
	SPEN	c.8075T>A	p.V2692D	-	-	0.49%	13/2679
	TNFAIP3	c.805+1_805+2insTGA	-	6.57%	39/594	9.44%	162/1716
	TNFAIP3	c.2080G>T	p.E694*	6.91%	39/564	7.83%	141/1801
	TNFAIP3	c.2350C>T	p.Q784*	-	-	2.45%	43/1756
	TP53	c.839G>A	p.R280K	5.91%	200/3384	8.68%	216/2488
	TP53	c.404G>A	p.C135Y	11.14%	142/1275	10.06%	175/1739
6	ACTB	c.142G>A	p.G48S	17.08%	2117/12396	1.66%	60/3616
	BTG1	c.92T>G	p.L31R	11.89%	240/2018	-	-
	BTG1	c.233C>T	p.P78L	19.02%	336/1767	-	-
	BTG1	c.138G>C	p.E46D	20.08%	200/996	-	-
	BTG1	c.108G>C	p.Q36H	20.97%	330/1574	-	-
	CD58	c.284T>G	p.L95*	20.09%	311/1548	-	-
	CD83	c.137_138insG	p.V47fs*11	14.82%	542/3656	-	-
	CD83	c.104G>A	p.C35Y	14.85%	598/4028	-	-
	HIST1H1E	c.140C>T	p.A47V	18.50%	810/4378	-	-
	HIST1H2AC	c.253C>T	p.Q85*	18.00%	770/4277	-	-
	HIST1H2AC	c.99delC	p.L34fs*23	21.44%	450/2099	-	-
	HIST1H2AM	c.193G>T	p.E65*	18.96%	229/1208	-	-
	HIST1H2BK	c.133G>C	p.V45L	12.88%	467/3625	-	-
	HIST1H2BK	c.148C>T	p.H50Y	13.02%	375/2881	-	-
	NFKBIA	c.205C>T	p.Q69*	15.71%	386/2457	-	-
	NFKBIA	c.185delG	p.G62fs*28	23.21%	688/2964	-	-
	TNFAIP3	c.982G>C	p.A328P	8.94%	68/761	-	-
	ZFP36L1	c.587C>A	p.P196H	12.22%	290/2374	-	-
84	ACTB	c.94C>T	p.P32S	28.03%	97/346	11.68%	48/411
	BCL6	c.1675G>C	p.G559R	50.89%	1976/3883	14.26%	937/6572
	BCL6	c.128T>G	p.F43C	49.04%	1256/2561	31.01%	1536/4954
	HIST1H2AM	c.346C>G	p.L116V	-	-	14.03%	452/3222
	HIST1H2BK	c.260G>C	p.R87P	-	-	7.62%	118/1548
	IRF8	c.131G>C	p.G44A	27.63%	334/1209	3.92%	138/3519
	IRF8	c.272A>C	p.D91A	44.04%	839/1905	12.66%	555/4383
	IRF8	c.313G>A	p.E105K	42.70%	798/1869	11.63%	450/3869
	MYD88	c.656C>G	p.S219C	44.00%	1534/3486	-	-
	MYD88	c.719T>C	p.M240T	-	-	17.46%	838/4799
	SF3B1	c.28+1G>T	-	5.85%	147/2511	-	-
	SGK1	c.1023G>T	p.E341D	-	-	5.47%	188/3439
	STAT3	c.1229A>C	p.H410P	23.01%	249/1082	-	-
	STAT3	c.1840A>C	p.S614R	-	-	11.92%	446/3742
	TMEM30A	c.281G>T	p.C94F	-	-	4.19%	100/2389
	TP53	c.614A>C	p.Y205S	64.85%	666/1027	-	-
	TP53	c.400T>A	p.F134I	-	-	11.54%	262/2271
	ZFP36L1	c.57+1G>A	-	45.91%	1004/2187	13.06%	217/1661
87	PLCG2	c.3431A>G	p.D1144G	29.21%	434/1486	-	-
34	BRAF	c.715C>T	p.R239*	3.87%	18/465	-	-
	HIST1H1C	c.523A>C	p.K175Q	-	-	8.4%	180/2148
	HIST1H1C	c.362A>C	p.K121T	-	-	1.6%	33/2043
	KMT2D	c.13081_13082insTG	p.A4361fs*24	-	-	12.4%	293/2356

	KMT2D	c.5065C>T	p.R1689C	-	-	0.9%	18/1932
	NFKBIA	c.198G>A	p.W66*	-	-	8.8%	32/364
	PIM1	c.550C>T	p.L184F	-	-	11.0%	197/1789
	SPEN	c.6254_6256delTAG	p.L2085_A2086delinsS	-	-	0.8%	19/2257
	TNFAIP3	c.832_833delAG	p.D279fs*5	-	-	25.3%	437/1725
	TP53	c.725G>A	p.C242Y	-	-	33.0%	771/2337
025	ACTB	c.1021A>G	p.I341V	17.50%	28/160	-	-
	HIST1H1E	c.122delC	p.E42fs*47	-	-	1.70%	62/3653
030	CD70	c.196+1G>A	-	52.26%	602/1152	-	-
	CD79B	c.552+2T>A	-	21.99%	419/1905	-	-
	HIST1H1C	c.194C>T	p.A65V	21.42%	921/4300	-	-
	HIST1H1C	c.124G>A	p.E42K	20.94%	768/3667	-	-
	HIST1H1D	c.571G>A	p.A191T	17.36%	516/2973	-	-
	HIST1H1E	c.367G>A	p.A123T	23.58%	1410/5980	-	-
	HIST1H2AM	c.379G>T	p.A127S	20.59%	561/2724	-	-
	HIST1H2BC	c.259C>T	p.R87C	18.01%	476/2643	1.31%	17/1302
	MYD88	c.656C>G	p.S219C	24.86%	1034/4159	-	-
	PIM1	c.521G>A	p.G174D	21.71%	647/2980	-	-
	SGK1	c.751C>T	p.H251Y	19.68%	109/554	-	-
	STAT3	c.1919A>T	p.Y640F	21.68%	137/632	-	-
	ZFP36L1	c.609C>G	p.S203R	21.37%	479/2241	-	-
	ZFP36L1	c.466G>C	p.E156Q	23.67%	835/3528	-	-
	ZFP36L1	c.277G>T	p.E93*	20.85%	519/2489	-	-
021	BTG1	c.109C>G	p.L37V	14.15%	176/1244	-	-
	HIST1H1E	c.14C>T	p.A5V	50.63%	283/559	-	-
	IRF8	c.1271T>A	p.I424N	18.73%	62/331	-	-
	PLCG2	c.731A>G	p.H244R	60.27%	264/438	-	-

Supplementary Figure S1. Pie chart illustrating the number of patients in each category: patients with the same IG clone identified in tumor biopsy and plasma ctDNA, patients only studied in the plasma compartment, and subgroups of patients excluded from MRD analysis due to the absence or unsuitability of the IG marker for subsequent analysis.

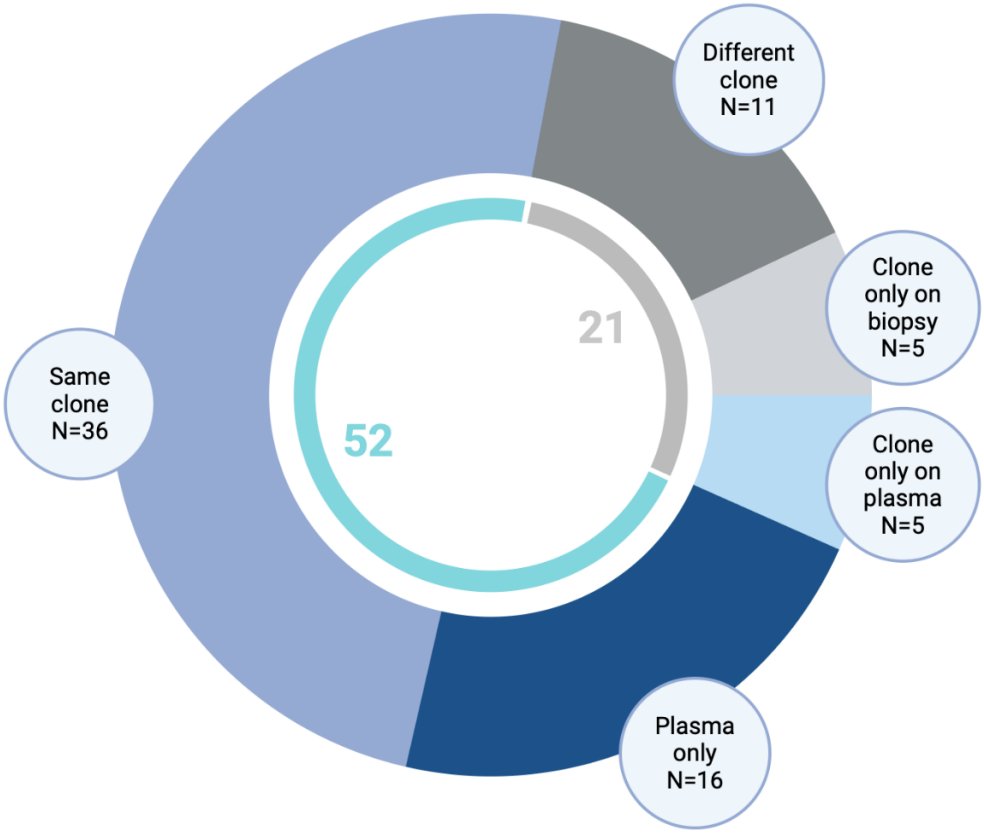

Supplementary Figure S2. Kaplan-Meier curve of PFS stratified according to whether a negative MRD on ctDNA was achieved or not at (A) cycle 2, day 1 (C2D1) and (B) cycle 4, day 1 (C4D1).